PROCEEDINGS OF SCIENCE

A leptonic model for the TeV γ-ray emission around Westerlund 1

Lucia Härer,[a,*] **Brian Reville,**[a] **Jim Hinton,**[a] **Lars Mohrmann**[a] **and Thibault Vieu**[a]

[a] *Max-Planck-Institut für Kernphysik, Saupfercheckweg 1, 69117 Heidelberg, Germany*

E-mail: lucia.haerer@mpi-hd.mpg.de

Young massive stellar clusters have come increasingly into the focus of discussions about the origin of PeV cosmic rays. Recently, the High Energy Stereoscopic System (H.E.S.S.) observed high-energy γ-ray emission around the young massive stellar cluster Westerlund 1, characterised by an energy independent, ring-like shape slightly off-set from the cluster position. We investigate the origin of this emission by modelling hadronic and leptonic emission processes with the open GAMERA library, discussing particle acceleration sites and propagation effects. Our findings support a predominately leptonic origin of the emission and highlight how the cluster's radiative and mechanical feedback facilitates particle acceleration.

7th Heidelberg International Symposium on High-Energy Gamma-Ray Astronomy (Gamma2022)
4-8 July 2022
Barcelona, Spain

*Speaker

PoS(Gamma2022)152

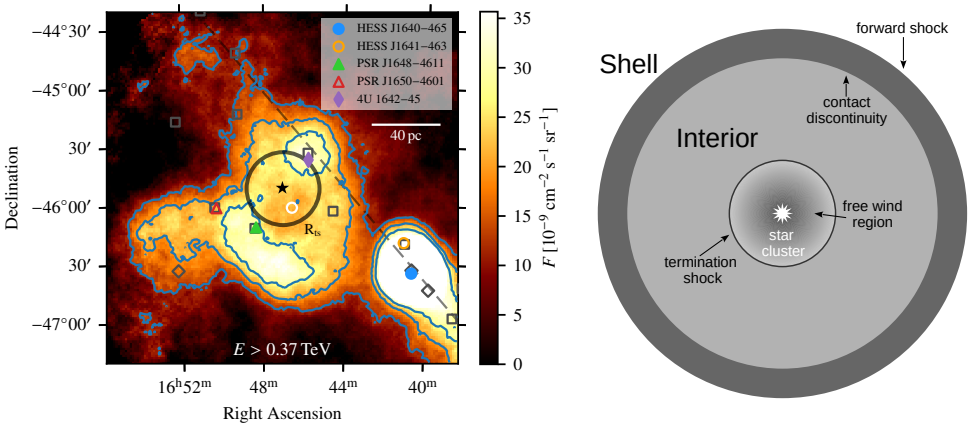

Figure 1: *Left*: H.E.S.S. observations of the Westerlund 1 region (Fig. 1b in [2]), overlayed with the predicted termination shock position assuming spherical symmetry. The star marks the cluster position, the small white circle the center point of the spherical geometry, and the dashed line the galactic plane. *Right*: structure of a bubble blown by a continuous wind from a central object. The interior is filled with hot, tenuous material. Note that in reality the bubble is often deformed due to inhomogeneities in the external medium.

1. TeV γ-rays around Westerlund 1 – Termination shock acceleration?

Young, massive stars have powerful, supersonic winds. In compact clusters, these winds and SN ejecta combine into a cluster wind, which blows a superbubble (SB). A basic model [1] of such a structure is shown in Fig. 1 (right). SBs enable particle acceleration, e.g., through large-scale shocks and turbulence. A recent analysis of H.E.S.S. data [2] revealed ring-like, energy and sub-region independent TeV γ-ray emission around Westerlund 1 (designated HESS J1646−458, Fig. 1, left), following the detection of the source in 2012 [3]. We propose particle acceleration at the cluster wind termination shock, $R_{\rm ts}$, as root cause of the emission and investigate the morphology and spectrum. In Westerlund 1, $R_{\rm ts}$ is expected to be at [1]

$$R_{\rm ts} \approx 20 \left(\frac{\xi_{\rm b}}{0.22}\right)^{-1/5} \left(\frac{\dot{M}}{5\times10^{-4}\,{\rm M_\odot\,yr^{-1}}}\right)^{3/10} \left(\frac{n_{\rm ext}}{100\,{\rm cm^{-3}}}\right)^{-3/10} \times \left(\frac{v_{\rm w}}{2500\,{\rm km\,s^{-1}}}\right)^{1/10} \left(\frac{t_{\rm sys}}{4\,{\rm Myr}}\right)^{2/5} {\rm pc}\,, \quad (1)$$

with the numerical prefactor $\xi_{\rm b}$ accounting for energy losses (see [4]), the cluster wind mass-loss rate and velocity, $\dot{M}$ and $v_{\rm w}$, the density outside the SB, $n_{\rm ext}$, and the age of Westerlund 1, $t_{\rm sys}$. This value coincides well with the inner radius of the emission (see Fig. 1, left). We do not model the acceleration process explicitly but assume an efficiency of conversation between the cluster wind power, $L_{\rm w}$, and the γ-ray luminosity above 1 GeV: $L_\gamma = \eta L_{\rm w} = \eta \times 0.5 \dot{M} v_{\rm w}^2$. We focus on leptonic emission processes, as hadronic models face severe difficulties (see Sect. 4). For an overview of other source candidates and acceleration sites see [2]. An analysis extending the work shown here can be found in [5]. All model parameters are summarised in Tab. 1.

As a prerequisite to the discussion of the leptonic model, we constrain the magnetic field in the acceleration region, $B_{\rm acc}$, and estimate the cluster photon field. Hillas' limit places a lower bound on the former for a given maximum particle energy, $E_{\rm max}$. The H.E.S.S. spectrum continues up to

Table 1: Input and dependent parameters of our Westerlund 1 γ-ray emission model. The values for $n_{\rm int}$, $R_{\rm ts}$, and $R_{\rm b}$ are calculated according to [1].

Input parameters			Dependent parameters		
Par.	Value	Description	Par.	Value	Description
$t_{\rm sys}$	4 Myr	cluster age	$n_{\rm int}$	$0.078\,{\rm cm^{-3}}$	density inside SB
d	3.9 kpc	cluster distance	$v_{\rm w}$	$2500\,{\rm km\,s^{-1}}$	cluster wind velocity
$L_{\rm w}$	$10^{39}\,{\rm erg\,s^{-1}}$	cluster wind power	$R_{\rm ts}$	20 pc	terminantion shock radius
$\dot{M}$	$5\times10^{-4}\,{\rm M_\odot\,yr^{-1}}$	mass-loss rate	$R_{\rm b}$	74 pc	SB radius
B	$2\,\mu$G	B-field (emission region)	$U_{\rm cl}$	$42\,{\rm eV\,cm^{-3}}$	cluster photon field energy density
$B_{\rm acc}$	$2\,\mu$G	B-field (acceleration region)			
$n_{\rm ext}$	$100\,{\rm cm^{-3}}$	density outside SB			
$L_{\rm bol}$	$10^{41}\,{\rm erg\,s^{-1}}$	cluster bolometric luminosity			
$T_{\rm eff}$	40,000 K	cluster effective temperature			

$E_\gamma \sim 80\,$TeV without a clear cut-off. The electrons should therefore reach at least $E_{\rm max} \sim 100\,$TeV. For the upstream field, Hillas limit reads [6]

$$B_{\rm acc} > \frac{E_{\rm max}c}{e v_{\rm w} R_{\rm ts}} \approx 0.7 \left(\frac{E_{\rm max}}{100\,{\rm TeV}}\right)\left(\frac{v_{\rm w}}{2500\,{\rm km\,s^{-1}}}\right)^{-1}\left(\frac{R_{\rm ts}}{20\,{\rm pc}}\right)^{-1}\mu{\rm G}\,. \tag{2}$$

In addition, efficient particle acceleration requires $M_{\rm A} \gg 1$, where the Alfvénic Mach number, $M_{\rm A}$, is the ratio of the wind velocity to the Alfvén speed, $v_{\rm A} = B_{\rm acc}/\sqrt{4\pi\rho(R_{\rm ts})}$. We express the gas density in terms of the mass-loss, $4\pi\rho(R)R^2 v_{\rm w} = \dot{M}$, with the radial distance from the cluster, R, and obtain $M_{\rm A} = v_{\rm w} v_{\rm A}^{-1} = \sqrt{\dot{M} v_{\rm w}} B_{\rm acc}^{-1} R_{\rm ts}^{-1}$. Hence, $B_{\rm acc}$ upstream of the shock has to be

$$B_{\rm acc} < 4.5 \left(\frac{R_{\rm ts}}{20\,{\rm pc}}\right)^{-1}\left(\frac{\dot{M}}{5\times10^{-4}\,{\rm M_\odot\,yr^{-1}}}\right)^{0.5}\left(\frac{M_{\rm A}}{10}\right)^{-1}\left(\frac{v_{\rm w}}{2500\ {\rm km\,s^{-1}}}\right)^{0.5}\mu{\rm G}\,, \tag{3}$$

adopting $M_{\rm A} = 10$ as a reference value for a strong shock. Equation 2 and 3 show that $B_{\rm acc}$ is quite strongly constrained in our scenario, especially for a weak wind. We take $B_{\rm acc} = 2\,\mu$G as a fiducial value in the following. We consider inverse Compton (IC) scattering on the CMB, direct and dust-scattered starlight (following [7]) and the cluster photon field. Due to its large population of massive stars, which are bright and hot, the effective temperature of the cluster photon spectrum is set to $T_{\rm eff} = 40{,}000\,$K. The energy density is given by $U_{\rm cl} = L_{\rm bol}(4\pi r^2 c)^{-1} \approx 42(L_{\rm bol}/10^{41}\,{\rm erg\,s^{-1}})(R_{\rm ts}/20\,{\rm pc})^{-2}\,{\rm eV\,cm^{-3}}$, estimating the bolometric luminosity based on measured of stellar magnitudes [8–10].

2. Morphology

A unique feature of HESS J1646−458 is its ring-like, energy independent morphology. We model electron transport and cooling in the SB interior, assuming continuous injection at the termination shock. The cooling times for leptonic interactions are calculated using the `GAMERA`[1] library, which takes into account Klein-Nishina corrections. As Fig. 2 (left) shows, the cooling time in the TeV-band is below the age of the system by ∼2 orders of magnitude. The size of the source is set by the length particles are transported within the cooling time. Transport can occur either by

[1] http://libgamera.github.io/GAMERA/docs/main_page.html

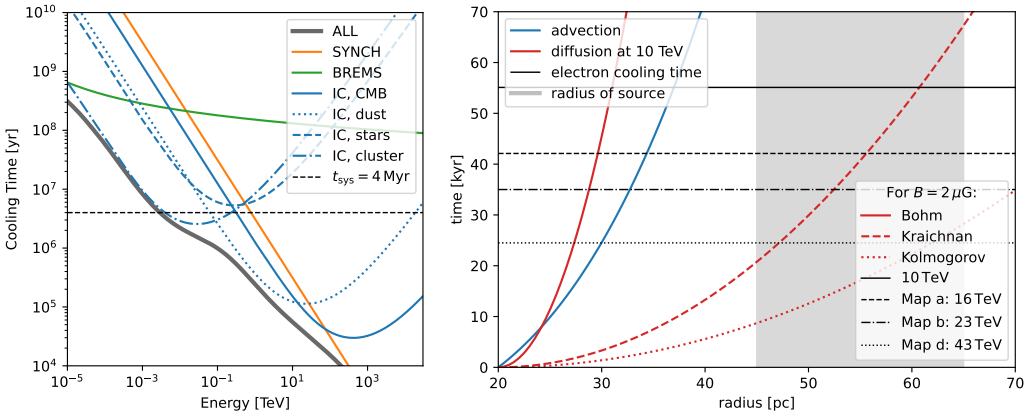

Figure 2: *Left:* Cooling times for leptonic interactions at $B = 2\,\mu$G inside the Westerlund 1 SB. *Right:* Advection and diffusion timescales compared to the electron cooling time. The dashed, dash-dotted, and dotted horizontal lines represent mean parent electron energies for H.E.S.S. maps with thresholds $E > 0.37$, >1, and >4.9 TeV (see [2], Fig. 3). The broad range given for the source's radius represents its asymmetry.

advection in the out-flowing wind or by diffusion. Figure 2 (right) shows the timescales for these processes, subdividing diffusion into a Bohm ($D \propto E^1$), Kraichnan ($D \propto E^{1/2}$), and a Kolmogorov case ($D \propto E^{1/3}$), where D is the diffusion coefficient, E the energy, and a turbulence injection scale of 1 pc is assumed.

If the magnetic field in the emission region is comparable to that in the acceleration region, i.e., $B \sim 2\,\mu$G, the transport should have a non-negligible advective component. For higher B, the cooling time is reduced, requiring the diffusive component to dominate. As diffusion is very sensitive to the energy scaling of the turbulence (see Fig. 2, right), the source size is consistent with several different scenarios. The characterisation of the H.E.S.S. emission as energy independent in based on maps with energy thresholds $E > 0.37$, >1, and >4.9 TeV (see [2], Fig. 3). For each map, one can obtain an average γ-ray energy, which in turn can be associated with an average parent electron energy. The cooling times at these energies are shown in Fig. 2 (right). The expected change in radius is ∼5 pc for advection, i.e., ∼4.4′ at 3.9 kpc, which is barely detectable and within the size variation seen in the maps. In addition, the energy scaling of D can counteract that of the cooling time in the diffusive transport.

3. Spectrum

We assume a cut-off powerlaw injection spectrum, $\mathrm{d}N/(\mathrm{d}E\mathrm{d}t) \propto E^{-\alpha_{\rm inj}} \exp(-E/E_{\rm cutoff})$, and use the `GAMERA` library[1] to calculate cooling and γ-ray emission. $E_{\rm cutoff}$ is obtained from equating the cooling and acceleration times in the Bohm limit. The latter is given by [11]

$$t_{\rm acc} \approx \frac{8 D_{\rm Bohm}}{v_{\rm w}^2} = \frac{8}{3}\frac{r_{\rm g} c}{v_{\rm w}^2} \approx 6.7 \left(\frac{E}{100\,\mathrm{TeV}}\right)\left(\frac{B_{\rm acc}}{2\,\mu\mathrm{G}}\right)^{-1}\left(\frac{v_{\rm w}}{2500\,\mathrm{km\ s^{-1}}}\right)^{-2} \mathrm{kyr}\,, \tag{4}$$

where $r_{\rm g}$ is the electron gyradius. Figure 3 (left) shows IC spectra for $B_{\rm acc} = 2\,\mu$G, which places the injection spectrum cut-off at 170 TeV. The IC model reproduces the spectral behaviour well for $\alpha_{\rm inj} = 2.1$–2.3 and requires a plausible efficiency, $\eta_{\rm IC} = 0.09$–0.28%. Higher values of $B_{\rm acc}$

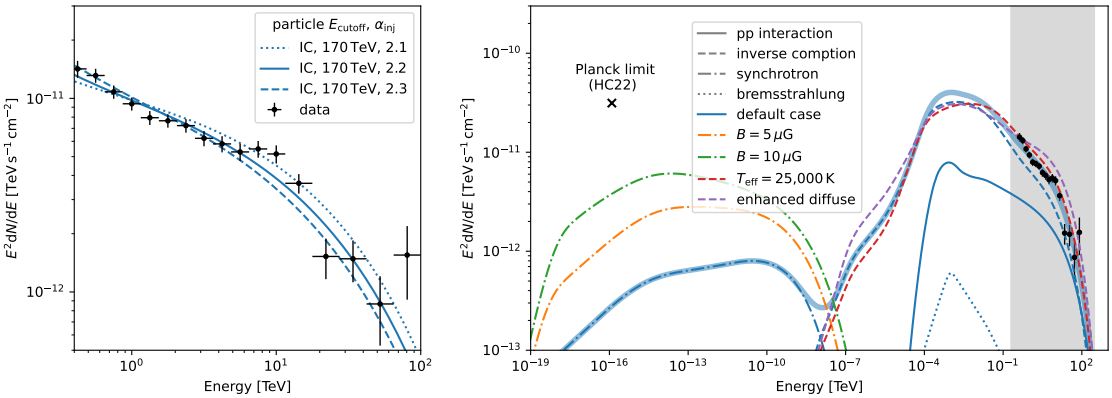

Figure 3: *Left:* IC models for the H.E.S.S. spectrum of the Westerlund 1 region. *Right:* Blue lines indicate the SED for the $\alpha_{\rm inj} = 2.2$ model (solid line on the left). Other colours show synchrotron emission for increased B, IC for $T_{\rm eff} = 25{,}000$ K, and an enhancement of the diffuse starlight and dust-scattered starlight by a factor of 3. The grey area marks the H.E.S.S. band. The *Planck* upper bound on the synchrotron flux inferred by [2] is indicated by the x-marker. The normalisation of all models matches that of the default case.

lead to lower cut-offs and systematically undershoot the highest energy data points, e.g., the cut-off for a 5 μG field, which roughly coincides with the upper limit from Eq. 3, is at 130 TeV. The right hand-side of Fig. 3 shows the multi-wavelengths SED model, which includes IC scattering, synchrotron emission and bremsstrahlung. In addition, we show a hadronic component, assuming proton acceleration at the termination shock, a 400 TeV cut-off in the injection spectrum, and $\eta_{\rm PP} = 100\eta_{\rm IC}$. The proton-proton (PP) emission is significantly below the IC, unless efficiencies close to 100% are assumed, which can be considered unrealistic. This result mainly stems from the low density inside the SB cavity, $n_{\rm int} < 0.1$ cm^{-3}. We vary photon field parameters and the magnetic field in the SED model (non-blue lines in Figure 3, right). The slope and shape of the spectrum in the H.E.S.S. band change slightly if the cluster effective temperature is reduced compared to the previously assumed $T_{\rm eff} = 40{,}000$ K or diffuse photon fields are enhanced. The latter could be a consequence of UV starlight form the cluster being reprocesses by dust. Higher values of B increase the synchrotron flux. [2] obtained an upper bound on this component from *Planck* data. Even for the 10 μG case, our model is consistent with the bound.

4. Discussion and conclusion

We interpret the γ-ray emission around Westerlund 1 in terms of particle acceleration at the cluster wind termination shock. Spectrum and morphology are consistent with IC scattering of energetic electrons on the ambient photon fields, which include the CMB, diffuse starlight and dust-scattered starlight, and UV emission from the cluster. Theoretical considerations constrain the acceleration region magnetic field to ~0.7–4.5 μG. In addition, we note that values larger than ~2 μG place the cut-off in the particle injection spectrum too low. With this constraint, the leptonic model predicts all features of the emission very well.

To complete the picture, we briefly highlight the key arguments that speak against a hadronic interpretation. A comprehensive discussion can be found in [5]. First, efficiencies close to 100%

would be required to reproduce the observed flux level, as demonstrated in Sect. 3, unless a spectral break not far below the H.E.S.S. band is present. Second, the PP cooling time is of the order of ~500 Myr, which is far longer than the age of the system. Advection in the out-flowing wind therefore carries protons inevitably out to the SB shell (cf. timescales in Fig. 2). Such a scenario would require a very high external density, ~300 cm^{-3}, to restrict the SB size to the size of the H.E.S.S. emission region. In addition, protons would be expected to diffuse into the dense shell, which should be clearly visible in γ-rays. We hope that future observatories such as CTA and SWGO will reduce the uncertainty in the spectrum above 20 TeV, as the position of the cut-off is a vital signature for acceleration and emission models.

References

[1] R. Weaver, R. McCray, J. Castor, P. Shapiro and R. Moore, *Interstellar bubbles. II. Structure and evolution.*, *APJ* **218** (1977) 377.

[2] F. Aharonian, H. Ashkar, M. Backes, V. Barbosa Martins, Y. Becherini, D. Berge et al., *A deep spectromorphological study of the γ-ray emission surrounding the young massive stellar cluster Westerlund 1*, *A&A* **666** (2022) A124 [2207.10921].

[3] A. Abramowski, F. Acero, F. Aharonian, A.G. Akhperjanian, G. Anton, S. Balenderan et al., *Probing the extent of the non-thermal emission from the Vela X region at TeV energies with H.E.S.S.*, *A&A* **548** (2012) A38 [1210.1359].

[4] T. Vieu, S. Gabici, V. Tatischeff and S. Ravikularaman, *Cosmic ray production in superbubbles*, *MNRAS* **512** (2022) 1275 [2201.07488].

[5] L.K. Härer, B. Reville, J. Hinton, L. Mohrmann and T. Vieu, *Understanding the TeV γ-ray emission surrounding the young massive star cluster Westerlund 1*, *submitted to A&A* (2022) .

[6] A.M. Hillas, *The Origin of Ultra-High-Energy Cosmic Rays*, *Annual review of astronomy and astrophysics* **22** (1984) 425.

[7] C.C. Popescu, R. Yang, R.J. Tuffs, G. Natale, M. Rushton and F. Aharonian, *A radiation transfer model for the Milky Way: I. Radiation fields and application to high-energy astrophysics*, *MNRAS* **470** (2017) 2539 [1705.06652].

[8] J.S. Clark, I. Negueruela, P.A. Crowther and S.P. Goodwin, *On the massive stellar population of the super star cluster Westerlund 1*, *A&A* **434** (2005) 949 [astro-ph/0504342].

[9] P.A. Crowther, L.J. Hadfield, J.S. Clark, I. Negueruela and W.D. Vacca, *A census of the Wolf-Rayet content in Westerlund 1 from near-infrared imaging and spectroscopy*, *MNRAS* **372** (2006) 1407 [astro-ph/0608356].

[10] I. Negueruela, J.S. Clark and B.W. Ritchie, *The population of OB supergiants in the starburst cluster Westerlund 1*, *A&A* **516** (2010) A78 [1003.5204].

[11] L.O. Drury, *REVIEW ARTICLE: An introduction to the theory of diffusive shock acceleration of energetic particles in tenuous plasmas*, *Reports on Progress in Physics* **46** (1983) 973.